The Kolmogoroff $r^{2/3}$ law

T. D. Dickey[a] and G. L. Mellor

Geophysical Fluid Dynamics Program, Princeton University, Princeton, New Jersey 08544
(Received 23 June 1978; final manuscript received 22 February 1979)

The Kolmogoroff $r^{2/3}$ law has been rederived from high wavenumber universal spectra and an additive constant has been obtained as a function of α, the empirical constant in the $r^{2/3}$ law. The value of α is uncertain. However, values determined from both structure function data and spectral density data have been collected and plotted as a function of Reynolds number. Although the results may be of more general interest, the original motivation for this study was to provide a diagnostic tool for evaluating the turbulent energy dissipation rate from correlation data (much as wall shear stress is evaluated from velocity profile data using the law of the wall). The technique for this procedure is illustrated.

I. INTRODUCTION

Our motivation for this paper resides in a need, perceived during the course of some experimental research at Princeton, to interpret velocity correlation data obtained with particle tracers in homogeneous turbulence. In this experiment, details of the correlation function can be obtained for small values of the separation distance but not the very small values governed by viscosity. Nevertheless, a goal would be to infer details for small r from universal similarity by matching data to the Kolmogoroff $r^{2/3}$ law. In principle, one could also deduce the turbulence dissipation much as the wall shear stress is deduced for velocity profile data in the logarithmic law of the wall region[1] where data in the viscous region are difficult to resolve. And, just as it is necessary to know the additive constant in the law of the wall, so it is necessary to know the additive constant in the Kolmogoroff $r^{2/3}$ law. We find from high wavenumber, universal spectra that the latter can be functionally related to α, the empirical coefficient of $(\epsilon r)^{2/3}$, where ϵ is the energy dissipation and r is the correlation separation distance.

Data at Reynolds numbers of $R_\lambda \approx 200$ and lower are not close to the asymptotic large Reynolds number case. Still, as a practical matter, one can also describe these data with an $r^{2/3}$ law where, however, it appears that α decreases as R_λ decreases. Values of α from the classical, low Reynolds number data of Batchelor and Townsend[2] and Stewart and Townsend[3] have therefore been determined.

The high Reynolds number correlation data of Van Atta and Chen[4] have been re-examined. From these data we obtain $\alpha \simeq 0.73$ instead of 0.58 according to their interpretation; the new figure is more in agreement with the value, $\alpha \simeq 0.70$, obtained from companion spectral data. Although sparse, the correlation data provide an apparently consistent Reynolds number dependent determination of α. However, if, in addition, values of α determined from numerous spectral density data are added, considerable scatter is introduced. Nevertheless, the final result is, it is believed, useful and instructive.

[a]Present address: Institute for Marine and Coastal Studies and Department of Geological Sciences, University of Southern California, University Park, Los Angeles, Calif. 90007.

II. ANALYSIS

The velocity correlation function is related to the one-dimensional spectral density function, $\phi(k)$ where k is the wavenumber, according to

$$\overline{uu'} = \int_0^\infty \phi(k) \cos kr \, dk, \qquad (1)$$

where the turbulent intensity $\bar{u}^2 \equiv \int_0^\infty \phi(k)\,dk$. $\overline{uu'}$ is the velocity correlation function and r, the distance separating u and u'. The relative correlation function or structure function is

$$\bar{u}^2 - \overline{uu'} = \int_0^\infty \phi(k)(1 - \cos kr)\, dk. \qquad (2)$$

According to Kolmogoroff's similarity hypothesis,

$$\phi = \alpha \epsilon^{2/3} k^{-5/3} \qquad (3)$$

in the inertial subrange, $k_0 \ll k \ll k_\nu$, where k_0^{-1} is the length scale of the energy containing eddies and

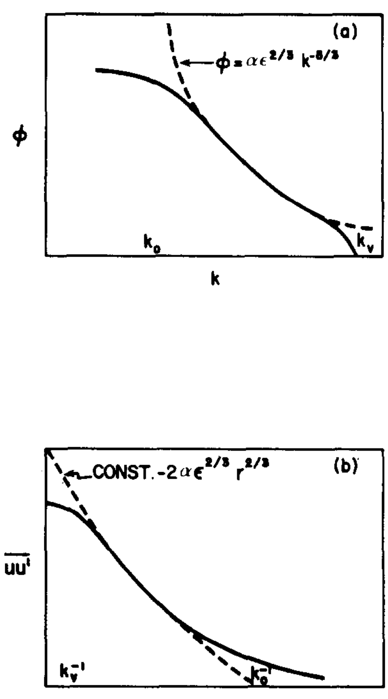

FIG. 1. Illustrative sketches of spectral density and correlation functions.

0031-9171/79/061029-04$00.90

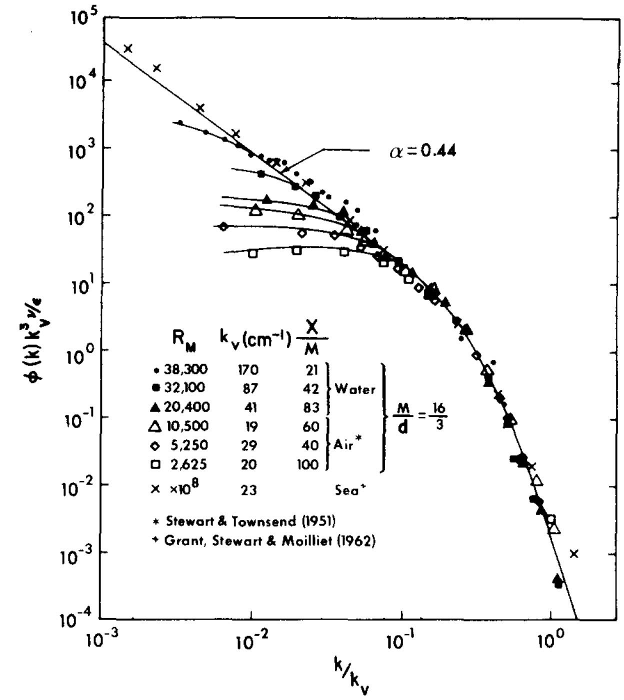

FIG. 2. Nondimensional spectral density versus nondimensional wavenumber. M/d is the ratio of mesh size to bar diameter (from Gibson and Schwarz[5]).

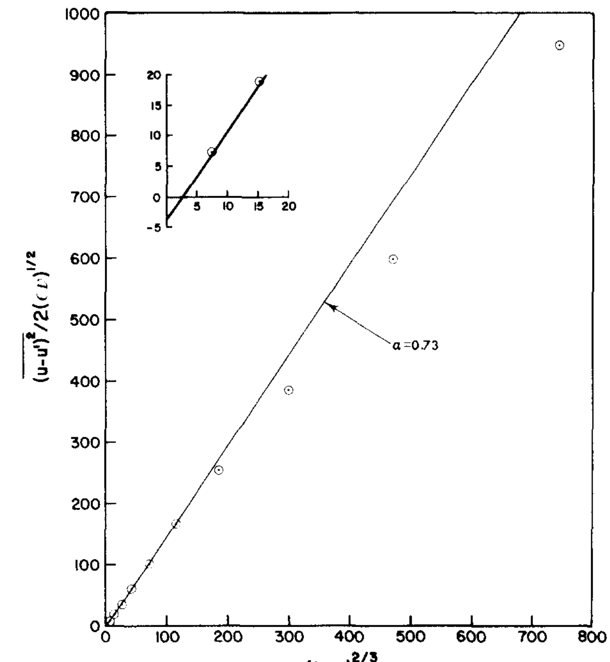

FIG. 4. Nondimensional relative turbulence velocity correlation function versus nondimensional separation distance. Data are from Van Atta and Chen[4] for the case $U = 11$ m/sec and $z = 23$ m. Insert shows intercept $-F(\alpha) = -3.69$.

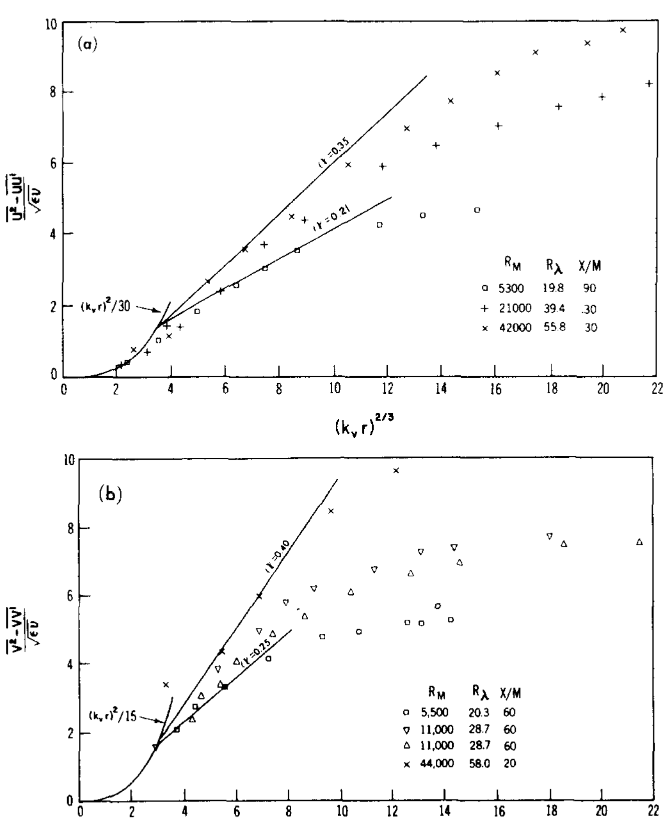

FIG. 3. Low Reynolds number structure function data compared to (a) longitudinal structure functions. The data are from Stewart and Townsend[3]. (b) Lateral structure functions for which one must replace α by $4/3\alpha$ in Eq. (6a). The data are from Batchelor and Townsend[2]. R_M is the mesh Reynolds number, $U_g M/\nu$ where U_g is the grid velocity and M is the grid mesh size.

$k_v^{-1} = (\nu^3/\epsilon)^{1/4}$, the small scale, dissipation length scale. Also, ν is the kinematic viscosity, ϵ is the energy dissipation rate and α is an empirical constant.

In Figs. 1(a) and 1(b), the behavior of spectral density and correlation functions are sketched as are approximate locations of k_0 and k_v. We now obtain the $r^{2/3}$ relation shown as a dashed line in Fig. 1(b). First, rewrite (2) according to

$$\overline{u^2} - \overline{uu'} = \int_0^{k_I} (\phi(k) - \alpha\,\epsilon^{2/3} k^{-5/3})\,(1 - \cos kr)\,dk + \int_0^{\infty} \alpha\,\epsilon^{2/3} k^{-5/3}\,(1 - \cos kr)\,dk + \int_{k_I}^{\infty} (\phi(k) - \alpha\,\epsilon^{2/3} k^{-5/3})\,(1 - \cos kr)\,dk\,,$$

where k_I is in the inertial subrange. The second integral is easily evaluated to be $2\alpha(\epsilon r)^{2/3}$. We next define

$$\tilde{k} \equiv k/k_0\,, \tag{4a}$$

$$\tilde{r} \equiv k_0 r\,, \tag{4b}$$

$$\hat{k} \equiv k/k_v\,, \tag{4c}$$

$$\hat{r} \equiv k_v r\,, \tag{4d}$$

so that

$$\frac{\overline{u^2} - \overline{uu'}}{(\epsilon\nu)^{1/2}} = \left(\frac{k_v}{k_0}\right)^{2/3} \int_0^{\tilde{k}_I} (\tilde{\phi}(\tilde{k}) - \alpha\tilde{k}^{-5/3})\,(1 - \cos\tilde{k}\tilde{r})\,d\tilde{k} + 2\alpha\hat{r}^{2/3} + \int_{\hat{k}_I}^{\infty} (\hat{\phi}(\hat{k}) - \alpha\hat{k}^{-5/3})\,(1 - \cos\hat{k}\hat{r})\,d\hat{k}\,, \tag{5}$$

where $\tilde{\phi} \equiv \phi k_0^{5/3}/\epsilon^{2/3}$ and $\hat{\phi} \equiv \phi k_v^{5/3}/\epsilon^{2/3}$. We note that $\tilde{k}_I$ may be set at any value so long as the integrand vanishes in the first integral for $\tilde{k} > \tilde{k}_I$ whereas $\hat{k}_I$ may be set at any value so long as the integrand in the last integral vanishes for $\hat{k} < \hat{k}_I$. (Figure 2 suggests the value $\hat{k}_I \lesssim 0.1$.)

We now wish to obtain an asymptotic approximation to (5) valid for small $\tilde{r}$ [so that the first integral in (5) vanishes] and, at the same time, valid for large $\hat{r}$. Conceptually, this may be achieved by fixing r while k_v increases and k_0 decreases. Formally, we set $\tilde{r} = O(\delta^{1/2})$ and $\hat{r} = O(\delta^{-1/2})$ and then let $\delta \equiv k_0/k_v \to 0$. Then, asymptotically, the first integral in (5) vanishes since $1 - \cos \tilde{k}\tilde{r} = \tilde{k}\, O(\delta)$. In the second integral, that part of the integrand that contains $\cos \hat{k}\hat{r}$ makes no contribution as $\hat{r} = O(\delta^{-1/2}) \to \infty$. Thus, we obtain

$$(\overline{u}^2 - \overline{uu'})/(\epsilon\nu)^{1/2} = -F(\alpha) + 2\alpha\hat{r}^{2/3}, \quad \hat{r} \to \infty \tag{6a}$$

where

$$F(\alpha) = -\int_{\hat{k}_I}^{\infty} (\hat{\phi}(\hat{k}) - \alpha\hat{k}^{-5/3})\, d\hat{k}. \tag{6b}$$

Note that, in the context of singular perturbation theory, (6a) may be regarded as the two largest terms of the outer asymptote of the "inner" function $(\overline{u}^2 - \overline{uu'})/(\epsilon\nu)^{1/2}$. It should also be noted that, if we assume that $\epsilon = O[k_0(\overline{u}^2)^{3/2}]$, then $\delta = O(R_\lambda^{-3/2})$ where

$$R_\lambda \equiv (\sqrt{\overline{u}^2}/\nu)\,\lambda\,, \tag{7a}$$

and λ is the Taylor microscale according to

$$15\,(\nu\overline{u}^2/\lambda^2) \equiv \epsilon = -15\,\nu\,(\partial^2\overline{uu'}/\partial r^2)_{r=0} \tag{7b}$$

Whereas (6) provides the large $\hat{r}$ behavior of the structure function, the small $\hat{r}$ behavior is obtained from (7b); thus,

$$(\overline{u}^2 - \overline{uu'})/(\epsilon\nu)^{1/2} \sim \tfrac{1}{30}\,\hat{r}^2, \quad r \to 0\,. \tag{8}$$

To obtain $F(\alpha)$, we refer to Fig. 2 where we reproduce the universal spectra compiled by Gibson and Schwarz.[5] Although the $k^{-5/3}$ portion is either absent or Reynolds number dependent, the spectrum for $\hat{k}$ greater than about 10^{-1} does appear insensitive to Reynolds number. Thus, letting $\hat{k}_I = 10^{-1}$, a numerical integration of (6b) yields

$$F(\alpha) = 6.96\,\alpha - 1.41\,. \tag{9}$$

III. DATA INTERPRETATION

We first consider classical, low Reynolds number correlation data in Figs. 3(a) and 3(b). Equations (6a) and (8) are also plotted for various α's and it is apparent that lower Reynolds numbers have a lesser slope. It may be argued that the lower Reynolds number data simply are too low for the existence of a significant region where (6a) might apply. This fact notwithstanding, we deem it useful to assign an apparent value of α which allows us to describe the small $\tilde{r}$ behavior.

We next consider data obtained in the atmospheric boundary layer over the ocean by Van Atta and Chen.[4] By examining correlation data for all available r on a log-log plot and apparently without cognizance of (6a), these authors concluded that $\alpha \simeq 0.58$ which was at variance with the value, 0.70, obtained from companion spectral data. However, in Fig. 4 we unambiguously obtain the value $\alpha \simeq 0.73$ where the $r^{2/3}$ intercept,

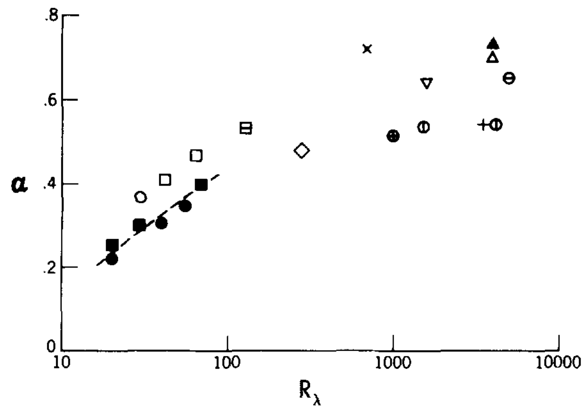

FIG. 5. The variation of α with R_λ. Solid symbols are velocity correlation data from Batchelor and Townsend[2] ■; Stewart and Townsend[3] ●; Van Atta and Chen[4] ▲. The remaining symbols are spectral data from Stewart and Townsend[3] ○, Comte-Bellot and Corrsin[6] □, Champagne *et al.*[7] ⊟, Schedvin *et al.*[8] ◇, Kistler and Vrebalovich[9] ×, Gibson *et al.*[10] ▽; Williams and Paulson[11] ⦶, Grant *et al.*[12] +, Van Atta and Chen[4] △, Sheih *et al.*[13] ⊖, Boston and Burling[14] ⦶. (Note, + reevaluated by Nasmyth[15]; □, ⊟ evaluated by Champagne[16]; ○, × evaluated by Schedvin *et al.*[8]).

$F(\alpha) = 3.7$, provided by (9) is also indicated experimentally.

If one stopped with the structure function data, one would have an apparently consistent, although data sparse, relationship between α and R_λ. However, we have also gathered values of α determined from spectral density data and these are plotted in Fig. 5 along with the spectral function data. In some cases the value represented in Fig. 5 is actually an average of many determinations in a given experiment. Additionally, for large but undetermined values of R_λ, the values $\alpha = 0.48 \pm 0.06$ and 0.57 ± 0.10 were obtained in Refs. 17 and 18, respectively.

The fact that values of α determined from structure function and spectral density data do not agree at low

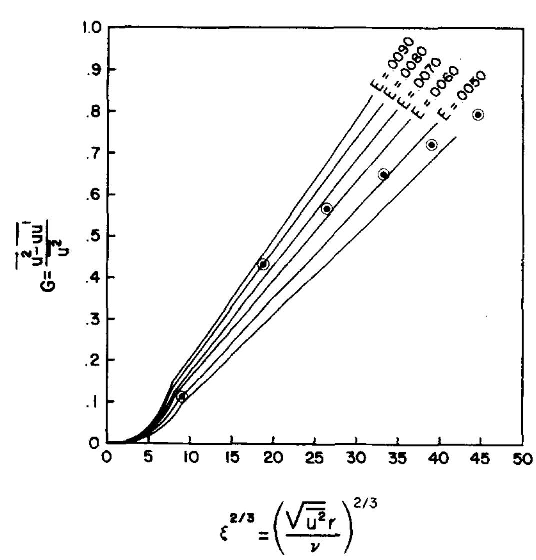

FIG. 6. Normalized relative velocity correlation function versus $\xi^{2/3}$, where ξ is a nondimensional separation distance. Data for $R_M = 48\,260$ and $X/M = 764$.

Reynolds number is not surprising; there is, in fact, some satisfaction in that they are reasonably close. The scatter in the large R_λ data, however, has been a long recognized difficulty. From Fig. 5, all that one can presume is that the asymptotocally large Reynolds number value of α lies in the range, $0.5 \lesssim \alpha \lesssim 0.7$. The correlation data and some of the spectral density data favor the upper value whereas most of the spectral data favor the lower value. Monin and Yaglom[19] discuss the issue thoroughly and also conclude that the weight of experimental data favors the lower value.

It should be noted that, in principle, one should not combine homogeneous decaying data with data obtained in geophysical boundary layers as has been done in Fig. 5. However, since α varies slowly for large variations in R_λ, the error should not be significant.

IV. A DIAGNOSTIC METHOD

We next illustrate how (6a) and (9) may be used as a diagnostic tool. First, Eq. (6a) can be normalized so that

$$G(\xi) \equiv (\overline{u}^2 - \overline{uu'})/\overline{u}^2 = 2\alpha E^{2/3}\xi^{2/3} - F(\alpha)E^{1/2}, \qquad (10)$$

where

$$E \equiv \epsilon\nu/(\overline{u}^2)^2, \qquad (11a)$$

$$\xi \equiv r\sqrt{\overline{u}^2}/\nu. \qquad (11b)$$

Similarly, $G(\xi)$ valid for small ξ can be obtained from (8). We have used the dashed line in Fig. 5 to obtain α as a function of R_λ.

The resultant family of $G(\xi)$ curves, parametric in E, are plotted in Fig. 6, along with a sample set of data. For the present illustrative purpose, it suffices to say that these data were obtained from particle trajectories in a tank of homogeneous, decaying turbulent water. (We plan to publish details of this experiment in the near future.) The correlation data are not very accurate; thus from Fig. 6 we estimate that $E = 0.0065 \pm 0.0015$.

In this particular example, had $F(\alpha)$ been unknown and arbitrarily set equal to zero, the value of E would have been estimated to be 25% lower.

A more accurate and independent measure of ϵ and therefore E was determined since $\overline{u}^2$, $\overline{v}^2$, and $\overline{w}^2$ were measured as a function of time. Then $\epsilon \equiv d[(\overline{u}^2 + \overline{v}^2 + \overline{w}^2)/2]/dt$ was obtained. Finally, through (11a), we obtain $E = 0.0060 \pm 0.0004$ for comparison with the value obtained from the diagnosis of the correlation data.

Note that the uncertainty in α becomes less important for smaller values of ξ since that portion of $G(\xi)$ obtained from (8) is exact as $\xi \to 0$.

V. CONCLUSION

The Kolmogoroff $r^{2/3}$ law is improved by addition of a constant. The final result is useful in interpreting old data and diagnosing new data. Data are assembled on a plot of α vs R_λ from a large number of experiments.

ACKNOWLEDGMENTS

Data obtained from Dr. Wilbur Chen and discussions with him contributed significantly to this paper.

This research was supported by the National Science Foundation under Grant No. ATM75-19326 and the Air Force Office of Scientific Research under Grant No. AFOSR-75-2756.

[1]F. H. Clauser, J. Atmos. Sci. 21, 91 (1954).
[2]G. K. Batchelor and A. A. Townsend, Proc. R. Soc. London Ser. A **190**, 534 (1947).
[3]R. W. Stewart and A. A. Townsend, Philos. Trans. A **243**, 359 (1951).
[4]C. W. Van Atta and W. Y. Chen, J. Fluid Mech. **44**, 145 (1970).
[5]C. H. Gibson and W. H. Schwarz, J. Fluid Mech. **16**, 365 (1963).
[6]G. Comte-Bellot and S. Corrsin, J. Fluid Mech. **48**, 273 (1971).
[7]F. H. Champagne, V. G. Harris, and S. Corrsin, J. Fluid Mech. **41**, 31 (1970).
[8]J. Schedvin, G. R. Stegen, and C. H. Gibson, J. Fluid Mech. **65**, 561 (1974).
[9]A. L. Kistler and T. Vrebalovich, J. Fluid Mech. **26**, 37 (1966).
[10]C. H. Gibson, G. R. Stegen, and R. B. Williams, J. Fluid Mech. **41**, 153 (1970).
[11]R. M. Williams and C. A. Paulson, J. Fluid Mech. **83**, 547 (1977).
[12]H. L. Grant, R. W. Stewart, and A. Moilliet, J. Fluid Mech. **12**, 241 (1962).
[13]C. M. Sheih, H. Tennekes, and J. L. Lumley, Phys. Fluids **14**, 201 (1971).
[14]N. E. J. Boston and R. W. Burling, J. Fluid Mech. **55**, 473 (1972).
[15]P. W. Nasmyth, Ph.D. dissertation, University of British Columbia (1970).
[16]F. H. Champagne, J. Fluid Mech. **86**, 67 (1978).
[17]S. Pond, S. D. Smith, P. F. Hamblin, and R. W. Burling, J. Atmos. Sci. **23**, 376 (1966).
[18]J. E. Paguin, and S. Pond, J. Fluid Mech. **50**, 257 (1971).
[19]A. S. Monin, and A. M. Yaglom, *Statistical Fluid Mechanics: Mechanics of Turbulence* (The MIT Press, Cambridge, Mass., 1975), Vol. 2, p. 479.